On the Kinematics of the Octopus's Arm

Yaron Levinson

Reuven Segev

Department of Mechanical Engineering,
Ben-Gurion University,
P.O. Box 653,
Beer-Sheva 84105, Israel

The kinematics of the octopus's arm is studied from the point of view of robotics. A continuum three-dimensional kinematic model of the arm, based on a nonlinear rod theory, is proposed. The model enables the calculation of the strains in various muscle fibers that are required in order to produce a given configuration of the arm—a solution to the inverse kinematics problem. The analysis of the forward kinematics problem shows that the strains in the muscle fibers at two distinct points belonging to a cross section of the arm determine the curvature and the twist of the arm at that cross section. The octopus's arm lacks a rigid skeleton and the role of material incompressibility in enabling the configuration control is studied. [DOI: 10.1115/1.4000528]

1 Introduction

This paper presents a kinematical model for the octopus's arm. The arm of an octopus is an efficient hyper-redundant manipulator and hence the motivation for studying it. We focus on the kinematic analysis of a three-dimensional continuum model. Of particular interest is the way the octopus uses the incompressibility of the arm to overcome the absence of a rigid skeleton. The following is a kinematical analysis that could suggest some applications in biomimetic robots. However, we do not consider specific applications to robots nor do we suggest technologies that may enable the construction of continuous robots having the kinematic model described below. A kinematic model of the octopus's arm having a finite number of degrees of freedom, and therefore, a lot simpler to implement, is presented in the first author's thesis [1].

In many cases, hyper-redundant robots are modeled and are designed as discrete mechanical systems [2–7]. However, particularly in the context of biomimetics, hyper-redundant robots are designed and are analyzed as continuous mechanical systems [8–16]. Accordingly, both discrete and continuous models of the octopus's arm have been studied.

Two-dimensional discrete kinematical and dynamical models for the octopus's arm are presented in Refs. [17,18]. In their study, the authors model the arm as an array of point masses interconnected by linear or nonlinear springs that represent the muscles. The incompressibility constraint is applied by preserving the area of each compartment created by four adjacent masses. The model considers external forces, such as gravity, drag, buoyancy, and internal forces, such as the muscles' active forces and the forces needed to preserve the area of the compartments.

Following studies such as in Refs. [19,20] on continuous models for hyper-redundant robots, Boyer et al. [21] used a geometrically exact theory of nonlinear beams to simulate the dynamics of swimming of an eel-like robot. In their analysis the robot is treated as a continuous series of infinitesimal sections. The deformation is defined by a homogeneous matrix $\mathbf{g}$ that describes the orientation and translation of each section. The authors write the differential equation for the homogeneous transformations of the cross section along the axis of the arm X in the form

$$\begin{bmatrix} \frac{\partial \mathbf{R}}{\partial X} & \frac{\partial \mathbf{d}}{\partial X} \\ 0 & 0 \end{bmatrix} = \begin{bmatrix} \mathbf{R} & \mathbf{d} \\ 0 & 1 \end{bmatrix} \begin{bmatrix} \hat{\mathbf{K}} & \mathbf{\Gamma} \\ 0 & 0 \end{bmatrix}$$

where $\mathbf{R}$ is the orientation matrix for the cross section, $\mathbf{d}$ is the position vector for the center of the cross section, $\mathbf{\Gamma} = \mathbf{R}^{\mathrm{T}}(\partial \mathbf{d}/\partial X)$, and $\hat{\mathbf{K}} = \mathbf{R}^{\mathrm{T}}(\partial \mathbf{R}/\partial X)$ is a skew-symmetric matrix whose components describe the bending and torsion of the robot. The first component of $\mathbf{\Gamma}$ describes the stretching of the centerline of the robot; the two remaining components describe the shear of the sections relative to one another. The dynamic model considers the swimming locomotion and the effect of forces caused by the flow.

The present work is similar to that of Boyer et al. [21], as we also used a geometrically nonlinear continuum theory of rods. However, our kinematic analysis of the octopus's arm studies what seems to us to be an essential aspect of the control of its configuration, namely, the role of an incompressibility constraint. Specifically, it is assumed here that the volume of any segment of the arm (bounded between two cross sections) remains fixed during a deformation.

It is noted that the equations governing the mechanics of pointwise incompressible rods are formulated and solved by Antman [22]. Antman did not present any application and his work is concerned with the kinematics of the cross sections for pointwise incompressible rods. As mentioned, we used a simplified theory where incompressibility is assumed to hold only for segments of the arm rather than pointwise.

The present kinematical model describes the relative rotations of the cross sections due to bending and torsion. As an additional kinematic constraint, we adopted a traditional hypothesis of the rod theory and did not consider transverse shear of the various cross sections.

Our objective is to study the kinematics of the octopus's arm from the point of view of robotics, namely, the inverse and direct kinematics problems. Thus, one has to define what parameters of the arm's configuration should be controlled and what are the actuation parameters. Subject to the constraints of the three-dimensional rod theory described, it is assumed here that it is necessary to control the configuration of the arm completely. In other words, rather than controlling a part of the arm, the analog of an end effector, the geometry of the entire centerline in space, and the twist of the arm about it are considered. This requirement is motivated by the existence of suction units along the entire length of the arm. The actuation parameters are the strains in the various muscle fibers of the arm. Thus, for the inverse kinematics problem, one seeks the strains in the various muscle groups that will induce a required configuration of the arm. For the forward kinematics problem, one seeks the configuration of the arm in-

Contributed by the Mechanisms and Robotics Committee of ASME for publication in the JOURNAL OF MECHANISMS AND ROBOTICS. Manuscript received May 7, 2009 final manuscript received September 29, 2009; published online November 24, 2009. Assoc. Editor: Jean-Pierre Merlet.

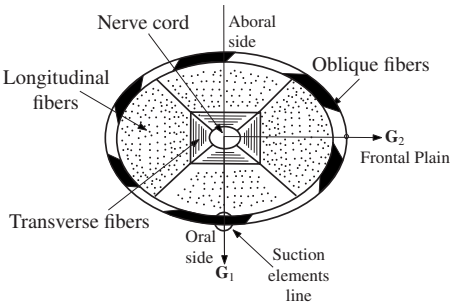

Fig. 1 A schematic cross section of an octopus's arm

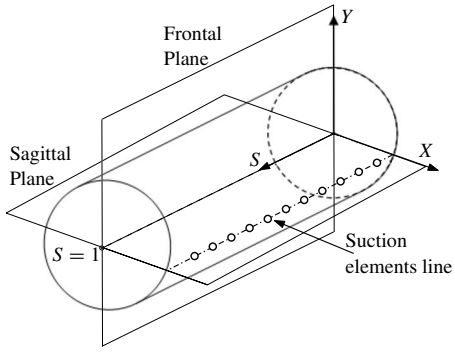

Fig. 2 The reference configuration of the arm

duced by the given strains in the muscle. An analysis of these two problems is presented in Sec. 5, following the introduction of the basic kinematic variables in Sec. 3 and the analysis of strain in Sec. 4.

2 Octopus's Arm Physiology: An Overview

Organs such as the mammalian tongue, the elephant's trunk, and the octopus's arms are termed *muscular hydrostats* [23]. They are characterized by their lack of vertebras and compressible cavities. The most important feature of muscular hydrostats is their relatively large bulk modulus that results from a dense musculature without any gas-filled cavities or large blood vessels [24]. This enables manipulation of an organ lacking any vertebrate skeleton by activating two or more muscle group simultaneously.

The octopus's arm consists of three primary muscle fiber groups surrounding a central axial nerve cord (Fig. 1): the longitudinal, transverse, and oblique or helicoidal muscles. The latter appear in both right and left handed coils.

The transverse muscle fibers are oriented in planes perpendicular to the axis of the arm. They are laid in an orthogonal array surrounding the axial nerve cord. Two bundles extend parallel to the lateral plane,[1] and two bundles are parallel to the frontal plane (see Fig. 2).

The longitudinal fibers surround the transverse fibers in four bundles: an oral, aboral, and two lateral bundles. The cross section area is larger in the aboral bundle, in comparison with the oral and lateral bundles. This enables the exertion of higher moments when the arm is bent aborally to reveal the suction line.

Helicoidal muscle fibers appear in three different layers: internal, median, and external. In every cross section, the three layers (or groups) spiral around the centerline both in right and left handed helices. Kier and Stella examined in Ref. [24] two octopus species and reported a mean pitch angle of 62 deg for external and median oblique muscle fibers. Internal oblique muscle fibers have a lower mean pitch angle that varies between the two species: 42 deg for octopus briareus and 56 deg for octopus digueti.

As the arm does not contain any rigid skeleton, control of the configuration is made possible by combining incompressibility with contractions of a number of muscle groups. In addition, the incompressibility property compensates for the inability of the muscle fibers to extend actively. For example, due to volume conservation, the arm will extend passively when the transverse muscles are contracted actively.

As another example, a contraction of the longitudinal muscle at the oral side will cause shortening of the arm and an increase in the cross section area. To avoid the contraction and create flexure, the cross section area is held fixed by contracting the transverse muscles. As a result of the arm's inability to change its volume, the aboral side must elongate and thus produce flexure of the arm in the sagittal plane.

[1]Note that in order to show the suction elements clearly, the sagittal plane is drawn horizontally in Fig. 2.

The role of the helicoidal muscle groups may be explained roughly as follows. Consider the arm in its straight unbent configuration. Assuming that the helicoidal muscles are in 45 deg to the centerline, the extension of the right handed helicoidal fibers and contraction of the same magnitude of the left handed helicoidal fibers will produce the shear strain needed for the right handed twist of the arm—the strain needed for the "adjacent" cross section to turn right relative to the "current" cross section. In general, muscle fibers do not extend actively. In the situation described above, the right handed fibers extend because of volume conservation.

As mentioned in the introduction, our objective in the paper is to give a robot kinematics model of the octopus's arm. In such a model, the strains in various muscle fiber groups make up the "joint variables." In such a model, for the inverse kinematics problem, one computes for the strains in the muscle fiber groups for a given configuration of the arm. In particular, the role of incompressibility is such a kinematic model will be studied.

3 Configurations of the Arm

3.1 Notation and Preliminaries. The reference configuration of the arm is assumed to be an elliptical cylinder in the vector space $\mathbb{R}^3$. Each material point in the arm is described by the reference coordinates $(X_1,X_2,X_3)=(X,Y,S)$ in some reference frame and it is assumed that at the reference configuration, the centerline occupies the points $(0,0,S)$ for $S\in[0,1]$ with the base of the arm being located at $S=0$. Thus, the centerline of the arm is situated along the $X_3=S$ axis and is set to be of a unit length for the sake of simplicity. The principal axes of the elliptical cross section of the cylinder are denoted as a_0 and b_0 and are in the directions of the X- and Y-coordinate axes, respectively. The suction elements are located on the points on the circumference of the cylinder for which $Y=0$ and $X=a_0$ (see Fig. 2).

The radius vector in the reference frame to typical material point of the arm is $\mathbf{R}=\mathbf{R}(X,Y,S)$ and the underformed centerline curve will be denoted as $\mathbf{R}_0(S)=\mathbf{R}(0,0,S)$. At each point in the reference state we may define the base vectors $\mathbf{G}_p=(\partial\mathbf{R}/\partial X_p)$. As the reference configuration is a right cylinder, the vectors $\{\mathbf{G}_p\}$ are orthonormal and are identical to the unit vectors along the reference coordinate axes.

The actual configurations of the arm take place in the physical space which we do not necessarily identify with the reference frame. The physical space is represented by a three-dimensional Euclidean space and it is assumed that a specific orthonormal frame is given. Thus, denoting the orthonormal base vector by $\mathbf{e}_i$ $(i=1,2,3)$, any point in space may be represented in the form $\mathbf{r}=x_i\mathbf{e}_i$, where summation on repeated indices is implied.

The deformed configuration of the arm is specified by a function $\mathbf{r}=\mathbf{r}(\mathbf{R})=\mathbf{r}(X,Y,S)$, giving the position in space corresponding to each material point $\mathbf{R}$ at the deformed configuration so that $x_i=x_i(X_p)$. For simplicity, the following is assumed:

ASSUMPTION 1. $\mathbf{r}(\mathbf{0})=\mathbf{0}$, *and the points* $(X,Y,0)$ *are mapped into* $(a_1X,a_2Y,0)$, *where* $a_1,a_2>0$.

In analogy with the notation we introduced earlier, the curve $\mathbf{r}_0(S)=\mathbf{r}(0,0,S)$ in the physical space will denote the centerline curve at the deformed state.

We now make the basic assumptions regarding the kinematics of the arm. These assumptions slightly generalize the traditional Euler–Bernoulli postulates for the rod theory in solid mechanics, where now in-plane deformations of the cross sections are admissible.

ASSUMPTION 2. *For each* $S_0\in[0,1]$, *the ellipse* $\{(X,Y,S_0),X^2/a_0^2+Y^2/b_0^2\leq 1\}$ *representing the cross section of the arm at* S_0 *is mapped onto an ellipse centered at* $\mathbf{r}_0(S_0)$.

ASSUMPTION 3. *The ellipse containing the points* $\mathbf{r}(X,Y,S_0)$ *is perpendicular to the deformed centerline at* $\mathbf{r}_0(S_0)$, *i.e.*

$$(\mathbf{r}(X,Y,S_0)-\mathbf{r}_0(S_0))\cdot\frac{d\mathbf{r}_0}{dS}(S_0)=0 \tag{3.1}$$

for all X,Y.

ASSUMPTION 4. *Vectors in the plane* $\{(X,Y,S_0)\}$ *are mapped linearly to the plane of the ellipse at* $\mathbf{r}_0(S_0)$, *i.e., for each* S_0 *the mapping*

$$\mathbf{R}(X,Y,S_0)-\mathbf{R}_0(S_0)\mapsto(\mathbf{r}(X,Y,S_0)-\mathbf{r}_0(S_0)) \tag{3.2}$$

is linear.

ASSUMPTION 5. *The lines* $\{(X,0,S_0)\}$ *and* $\{(0,Y,S_0)\}$ *are mapped to the principal axes of the ellipse* $\mathbf{r}(X,Y,S_0)$.

We will naturally refer to the points $\mathbf{r}(X,Y,S_0)$ as the cross section of the deformed arm at S_0. Thus, Assumption 1 implies that the cross section at $S_0=0$ is not translated, rotated, or twisted. It is just stretched or contracted along the X- and Y-directions. Assumptions 2 and 3 are the classical assumption of the rod theory that plane sections normal to the centerline remain plane and normal to the deformed centerline. Unlike the traditional Kirchhoff theory, we allow a cross section to deform in its plane. Assumption 4 implies that the in-plane deformation is homogeneous. In terms of the octopus's physiology, this implies uniform strain in the transverse fiber muscles. Furthermore, Assumption 5 implies that the X and Y are the principle axes of the in-plane linear strain, and as such, they remain perpendicular.

3.2 The Centerline Triads. For each point in the deformed arm, consider the base vectors

$$\mathbf{g}_p=\frac{\partial\mathbf{r}}{\partial X_p} \tag{3.3}$$

and note that

$$\mathbf{g}_p=\frac{\partial\mathbf{r}}{\partial X_p}=\frac{\partial\mathbf{r}}{\partial x_i}\frac{\partial x_i}{\partial X_p}=\frac{\partial x_i}{\partial X_p}\mathbf{e}_i \tag{3.4}$$

The vector $\mathbf{g}_p$ at point $\mathbf{r}_1=\mathbf{r}(\mathbf{R}_1)$ is tangent to the curve through $\mathbf{r}_1$, which contains the image of the curve $\mathbf{R}(X_p)=\mathbf{R}_1+X_{(p)}\mathbf{G}_{(p)}$ (no summation). Thus, for example

$$\mathbf{g}_3(0,0,S)=\frac{\partial\mathbf{r}}{\partial S}(0,0,S)=\frac{d\mathbf{r}_0}{dS}(S) \tag{3.5}$$

is tangent (not necessarily of unit length) to the deformed centerline $\mathbf{r}_0(S)$. In addition, the vectors $\mathbf{g}_1$ and $\mathbf{g}_2$ are tangent to the cross section of the deformed arm.

From Assumptions 4 and 5 it follows that the base vectors $\mathbf{g}_1$ and $\mathbf{g}_2$ are uniform and mutually perpendicular in any particular cross section. In each elliptical cross section of the deformed arm, $\mathbf{g}_1$ and $\mathbf{g}_2$ are parallel to the principal axes. These two vectors represent the directions of the two mutually perpendicular transverse muscle groups in the deformed arm. By Assumption 3, $\mathbf{g}_3(0,0,S)$ is perpendicular to both $\mathbf{g}_1$ and $\mathbf{g}_2$. We conclude that the triads $\mathbf{g}_p(0,0,S)$ contain mutually orthogonal vectors. The vectors $\mathbf{g}_p(X,Y,S)$ at points other than the centerline need not be perpendicular. If, for example, the deformed arm becomes conical, the longitudinal fibers are no longer parallel. It is noted that the base vectors are not necessarily of unit length due to the centerline extension and the change in the principal axes of the elliptic cross section.

We will refer to the triads $\mathbf{g}_p(0,0,S)$ as the centerline triads. It follows from Eq. (3.4) that at each S there is a linear mapping $T(S)$, whose matrix is $\partial x_i/\partial X_p(0,0,S)$, such that

$$\mathbf{g}_p(0,0,S)=T(S)_{ip}\mathbf{e}_i \tag{3.6}$$

It is recalled that according to the polar decomposition theorem, a nonsingular linear mapping T may be decomposed in the form

$$T=Q\circ U \tag{3.7}$$

where Q is an orthogonal mapping and U is a positive definite symmetric mapping. Applying this to the mappings $T(S)$, so that $T(S)=Q(S)\circ U(S)$, one can write for the centerline triads

$$\mathbf{g}_p(0,0,S)=Q(S)_{ij}U(S)_{jp}\mathbf{e}_i \tag{3.8}$$

Each of the triads $\{\mathbf{d}_j(S)\}$, defined by

$$\mathbf{d}_j(S)=Q(S)_{ij}\mathbf{e}_i \tag{3.9}$$

contains mutually orthogonal unit vectors. As the parameter S varies, the orthonormal triad rotates according to $Q(S)$ (see Fig. 3). In our case, as the vectors $\mathbf{g}_p(0,0,S)$ are mutually orthogonal, the polar decomposition is particularly simple. The vector $\mathbf{d}_j$ is simply the unit vector in the direction of the vector $\mathbf{g}_j$. The matrix Q_{ij} contains the components of $\mathbf{d}_j$ and the matrix U_{jp} is diagonal and contains the norms $\|\mathbf{g}_p\|$ of the vectors belonging to the centerline triad on its diagonal. The various $\{\mathbf{d}_i\}$ triads associated with the points $S\in[0,l]$ along the centerline will be referred to as the *orthonormal rod frames*.

It follows that

$$\mathbf{d}_p(S)=\frac{1}{\|\mathbf{g}_p\|}\mathbf{g}_p(0,0,S)\quad\text{(no summation)} \tag{3.10}$$

the unit vector $\mathbf{d}_3$ is tangent to the deformed centerline curve, and

$$\mathbf{g}_1(S)=a_1(S)\mathbf{d}_1(S),\quad a_1(S)=\|\mathbf{g}_1(0,0,S)\| \tag{3.11}$$

$$\mathbf{g}_2(S)=a_2(S)\mathbf{d}_2(S),\quad a_2(S)=\|\mathbf{g}_2(0,0,S)\| \tag{3.12}$$

Using $\mathfrak{s}$ for the arc length parameter for the deformed centerline and assuming naturally that $\mathfrak{s}(S)$ is a monotonically increasing function, it follows from Eq. (3.5) that the stretch or extension of the centerline is given by

$$\frac{d\mathfrak{s}}{dS}(S)=\|\mathbf{g}_3(0,0,S)\| \tag{3.13}$$

We denote the stretch of the arm's centerline as $\lambda(S)=\|\mathbf{g}_3(0,0,S)\|$ and the length of the deformed centerline as $l=\int\lambda dS$.

Using the centerline triads, our assumptions imply that the configuration of the arm may be represented by

$$\begin{aligned}\mathbf{r}(\mathbf{R})&=\mathbf{r}_0(S)+X\mathbf{g}_1(0,0,S)+Y\mathbf{g}_2(0,0,S)\\ \mathbf{r}(\mathbf{R})&=\mathbf{r}_0(S)+Xa_1(S)\mathbf{d}_1(S)+Ya_2(S)\mathbf{d}_2(S)\end{aligned} \tag{3.14}$$

3.3 The Extended Darboux Vector. As the parameter $\mathfrak{s}$ varies, the triad $\{\mathbf{d}_i\}$ undergoes a rigid motion. The origin of the triad is displaced tangent to the deformed centerline. The vectors $\mathbf{d}_i$ are rotated rigidly, as expressed by Eq. (3.9). As $\mathfrak{s}(S)$ was assumed to be monotonically increasing, one may consider the dependence $\mathbf{d}_i(\mathfrak{s})=\mathbf{d}_i(S(\mathfrak{s}))$.

Consider the rates

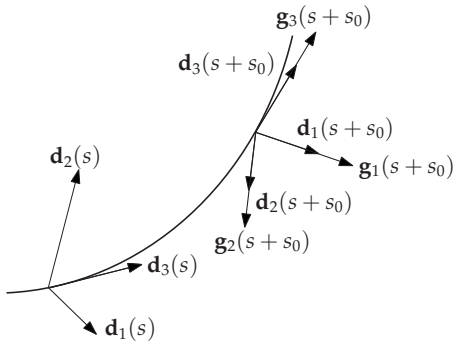

Fig. 3 The triads $\{\mathbf{g}_i\}$ and $\{\mathbf{d}_i\}$ (i=1,2,3)

$$\frac{d\mathbf{d}_i}{d\mathfrak{s}} = \frac{d\mathbf{d}_i}{dS}\frac{dS}{d\mathfrak{s}} = \frac{1}{\lambda}\frac{dQ(S)_{ji}}{dS}\mathbf{e}_j \tag{3.15}$$

These rotation rates may be represented by a vector $\mathbf{u}$, so that

$$\frac{d\mathbf{d}_i}{d\mathfrak{s}} = \mathbf{u} \times \mathbf{d}_i \tag{3.16}$$

The components of $\mathbf{u}$ may be found by dot multiplying Eq. (3.16) by $\mathbf{d}_j$ obtaining

$$\frac{d\mathbf{d}_i}{d\mathfrak{s}} \cdot \mathbf{d}_j = (\mathbf{u} \times \mathbf{d}_i) \cdot \mathbf{d}_j \tag{3.17}$$

Using ϵ_{ijk} to denote the permutation symbol, we have

$$\frac{d\mathbf{d}_i}{d\mathfrak{s}} \cdot \mathbf{d}_j = u_m \epsilon_{ijm}, \quad u_m = \frac{1}{2}\epsilon_{ijm}\frac{d\mathbf{d}_i}{d\mathfrak{s}} \cdot \mathbf{d}_j \tag{3.18}$$

It is straightforward to write similar expressions for the rates relative to the parameter S and write the relations between the two types of rates.

It is customary in rod theory [25] to denote the components of the vector $\mathbf{u}$ as $\{\kappa, \kappa', \tau\}^T$ so

$$\begin{Bmatrix} \kappa \\ \kappa' \\ \tau \end{Bmatrix} = \begin{Bmatrix} u_1 \\ u_2 \\ u_3 \end{Bmatrix} = \begin{Bmatrix} \dfrac{d\mathbf{d}_2}{d\mathfrak{s}} \cdot \mathbf{d}_3 \\ \dfrac{d\mathbf{d}_3}{d\mathfrak{s}} \cdot \mathbf{d}_1 \\ \dfrac{d\mathbf{d}_1}{d\mathfrak{s}} \cdot \mathbf{d}_2 \end{Bmatrix} \tag{3.19}$$

Denoting differentiation with respect to S by a prime, we immediately get by the chain rule

$$\mathbf{d}_i' = \lambda\frac{d\mathbf{d}_i}{d\mathfrak{s}} = \lambda\mathbf{u} \times \mathbf{d}_i \tag{3.20}$$

The linear mapping $\mathbf{\Omega}$ defined by

$$\mathbf{\Omega}(\mathbf{v}) = \lambda\mathbf{u} \times \mathbf{v} \tag{3.21}$$

is represented by the matrix

$$\lambda\begin{bmatrix} 0 & \tau & -\kappa' \\ -\tau & 0 & \kappa \\ \kappa' & -\kappa & 0 \end{bmatrix} \tag{3.22}$$

Thus, one has

$$\begin{Bmatrix} \mathbf{d}_1' \\ \mathbf{d}_2' \\ \mathbf{d}_3' \end{Bmatrix} = \mathbf{\Omega}\begin{Bmatrix} \mathbf{d}_1 \\ \mathbf{d}_2 \\ \mathbf{d}_3 \end{Bmatrix} \tag{3.23}$$

The components of the vector $\mathbf{u}$ may be interpreted as follows: κ and κ' represent the bending of the centerline about the axes $\mathbf{d}_1$ and $\mathbf{d}_2$, respectively, and τ is the torsion about the tangent to the curve $\mathbf{d}_3$. The parameter τ is different from the intrinsic torsion of the deformed centerline (described in the Appendix) as it accounts for the relative twist of the various cross sections of the arm. In addition, while the intrinsic torsion of a curve is not defined for the case where the curvature vanishes (see Appendix), τ is always well defined. It is noted that the rotation rate vector $\mathbf{u}$ is an extension of the Darboux vector used in differential geometry.

From the representation of the configuration in Eq. (3.14), as the centerline triads may be obtained from their derivatives through integration and using the initial conditions given by Assumption 1, we conclude that the collection of function $\{\kappa(S), \kappa'(S), \tau(S), \lambda(S), a_1(S), a_2(S)\}$ defines uniquely the configuration of an extensible rod under the assumptions made earlier. For example

$$\mathbf{r}_0(S) = \int_{\sigma=0}^{S} \lambda(\sigma)\mathbf{d}_3(\sigma)d\sigma \tag{3.24}$$

4 The Deformation Gradient and Strain

4.1 The Matrix of the Deformation Gradient. Equation (3.14) for the description of the configuration determines the position vector in the deformed state of a particle having reference coordinates (X, Y, S) by

$$\mathbf{r}(X, Y, S) = x_i\mathbf{e}_i = \mathbf{r}_0(S) + X\mathbf{g}_1(0,0,S) + Y\mathbf{g}_2(0,0,S)$$

We recall that the deformation gradient of solid mechanics is the linear mapping

$$\mathbf{F} = F_{ip}\mathbf{e}_i \otimes \mathbf{G}_p \tag{4.1}$$

represented by the matrix

$$F_{ip} = \frac{\partial x_i}{\partial X_p} \tag{4.2}$$

Thus, the first two columns of the deformation gradient matrix are given by

$$F_{i1}\mathbf{e}_i = \frac{\partial \mathbf{r}}{\partial X} = \mathbf{g}_1 \tag{4.3}$$

$$F_{i2}\mathbf{e}_i = \frac{\partial \mathbf{r}}{\partial Y} = \mathbf{g}_2 \tag{4.4}$$

and the third column is given by

$$F_{i3}\mathbf{e}_i = \frac{\partial \mathbf{r}_0}{\partial S} + X\frac{\partial \mathbf{g}_1}{\partial S} + Y\frac{\partial \mathbf{g}_2}{\partial S} = \lambda\mathbf{d}_3 + X\left(\frac{da_1}{dS}\mathbf{d}_1 + a_1\frac{d\mathbf{d}_1}{dS}\right) + Y\left(\frac{da_2}{dS}\mathbf{d}_2 + a_2\frac{d\mathbf{d}_2}{dS}\right) \tag{4.5}$$

For any particular S, one may choose the basis $\{\mathbf{e}_i\}$ in space to be identical to the triad $\{\mathbf{d}_i(S)\}$. Under this specific choice, the last expressions imply that the matrix of $\mathbf{F}(X, Y, S)$ assumes the form

$$[\mathbf{F}]_{\mathbf{d}}(X, Y, S) = \begin{bmatrix} a_1 & 0 & \dfrac{da_1}{dS}X - \tau a_2\lambda Y \\ 0 & a_2 & \tau a_1\lambda X + \dfrac{da_2}{dS}Y \\ 0 & 0 & \lambda - \kappa' a_1\lambda X + \kappa a_2\lambda Y \end{bmatrix} \tag{4.6}$$

where the dependence of the various variables on S was omitted on the right.

4.2 The Consequences of Incompressibility. As mentioned in Sec. 2, the octopus's arm is almost entirely composed of virtually incompressible muscle tissue. Indeed, in earlier treatments of octopus arm kinematics [24] it is assumed that the arm is incompressible. For the sake of simplicity, we assume the incompressibility constraint holds for segments of the arm rather than point-

wise. A theoretical treatment of rod theory, where the rod is assumed to be pointwise incompressible, was presented only recently in Ref. [22]. Thus, we make the following assumption:

ASSUMPTION 6. *The volume of any segment* $\{(X,Y,S)\}$ $(0 \le S_1 \le S \le S_2 \le 1)$ *of the arm does not change under deformation.*

It is noted that for a pointwise incompressibility constraint, the in-plane deformation of a cross section is not homogeneous [22]. Thus, pointwise incompressibility requirement would be inconsistent with our earlier assumptions.

Consider a volume element dV_0 containing a material point $\mathbf{R}$ and its image dV containing $\mathbf{r}(\mathbf{R})$. Then, using J for the determinant of the deformation gradient, one has $dV/dV_0 = J$. The volume V of a deformed segment of the arm is thus given as

$$V = \iiint J dX dY dS$$
$$V = \int_{S_1}^{S_2} a_1(S) a_2(S) \lambda(S) \pi a_0 b_0 dS \tag{4.7}$$

Assuming that the integrand in Eq. (4.7) is continuous, we conclude that a necessary and sufficient condition for the volume of every segment of the arm to remain unchanged, i.e., that $V = V_0 = \pi a_0 b_0 (S_2 - S_1)$, is

$$\lambda(S) = \frac{1}{a_1(S) a_2(S)}, \quad \forall\, S \in [0,1] \tag{4.8}$$

Since the last equation cannot determine a unique pair (a_1, a_2) we make the following assumption:

ASSUMPTION 7. *The arm preserves the initial ratio between the lengths of the principal axes of the elliptic cross section.*

We denote the abovementioned ratio as $r := (a_0/b_0)$. Consequently, $(a_0/b_0) = (a_1 a_0 / a_2 b_0)$, and so, $a_1(S) = a_2(S) = \mathfrak{a}(S)$.

4.3 Strain Analysis. Consider an infinitesimal vector

$$d\mathbf{X} = dX_p \mathbf{G}_p \tag{4.9}$$

originating at the point $\mathbf{R}$ in the reference configuration, whose image under the deformation is

$$d\mathbf{x} = dx_i \mathbf{e}_i = \frac{\partial x_i}{\partial X_p} dX_p \mathbf{e}_i = \mathbf{F}(d\mathbf{X}) \tag{4.10}$$

originating at $\mathbf{r}(\mathbf{R})$. It is convenient, and indeed of wide use in the mechanics of continuous media, to describe the extension of the element $d\mathbf{X}$ by the quantity

$$\tfrac{1}{2}[d\mathbf{x} \cdot d\mathbf{x} - d\mathbf{X} \cdot d\mathbf{X}] = \tfrac{1}{2}[\mathbf{F}^T\mathbf{F} - \mathbf{I}](d\mathbf{X}) \cdot d\mathbf{X} = \mathbf{E}(d\mathbf{X}) \cdot d\mathbf{X} \tag{4.11}$$

where

$$\mathbf{E} = \tfrac{1}{2}[\mathbf{F}^T\mathbf{F} - \mathbf{I}] \tag{4.12}$$

is the Lagrangian strain tensor.

This standard definition may be motivated intuitively using the special case of small deformations superimposed on the reference deformation as follows: If the vector $d\mathbf{X}$ is normalized to be of unit length, $\frac{1}{2}[d\mathbf{x} \cdot d\mathbf{x} - d\mathbf{X} \cdot d\mathbf{X}]$ is the linear approximation to the change in length of $d\mathbf{X}$ during the deformation.

Returning to the general case of large deformations, for a unit vector $\hat{\mathbf{n}}$ originating at (X,Y,S), it is natural to refer to

$$\epsilon_{\hat{\mathbf{n}}}(X,Y,S) = (\mathbf{E}(X,Y,S)\hat{\mathbf{n}}) \cdot \hat{\mathbf{n}} \tag{4.13}$$

as the *strain* at the point (X,Y,S) in the direction of $\hat{\mathbf{n}}$.

Once again, the Lagrangian strain tensor has a simpler expression when written relative to the orthonormal rod frame, and we have

$$[\mathbf{E}]_{\mathbf{d}} = \frac{1}{2}\begin{bmatrix} \mathfrak{a}^2 - 1 & 0 & \mathfrak{a}\left(\frac{d\mathfrak{a}}{dS}X - \mathfrak{a}\lambda Y\tau\right) \\ 0 & \mathfrak{a}^2 - 1 & \mathfrak{a}\left(\frac{d\mathfrak{a}}{dS}Y + \mathfrak{a}\lambda X\tau\right) \\ \mathfrak{a}\left(\frac{d\mathfrak{a}}{dS}X - \mathfrak{a}\lambda Y\tau\right) & \mathfrak{a}\left(\frac{d\mathfrak{a}}{dS}Y + \mathfrak{a}\lambda X\tau\right) & (\mathfrak{a}Y\lambda\kappa - \mathfrak{a}X\lambda\kappa' + \lambda)^2 + \left(\frac{d\mathfrak{a}}{dS}Y + \mathfrak{a}\lambda X\tau\right)^2 + \left(\frac{d\mathfrak{a}}{dS}X - \mathfrak{a}\lambda Y\tau\right)^2 - 1 \end{bmatrix} \tag{4.14}$$

It is noted that for $X = Y = 0$, the mapping $\mathbf{F}$ becomes the mapping T of Eq. (3.6). The strain $\mathbf{E}$ at the centerline is given by $(U^T \circ U - I)/2 = (T^T \circ T - I)/2$, where U is the positive definite component of the decomposition in Eq. (3.7).

5 Manipulator Kinematic Analysis

In this section we consider the octopus's arm as a manipulator and we study its kinematic properties, specifically, the inverse and direct kinematics. In order to perform such an analysis, one has to define what parameters of the configurations should be controlled. The arm is used as a tool along its entire length and the objective is to bring the suction elements into contact with some surface in such a way that the arm and the surface are tangent along the contact line. Thus, the manipulator kinematic analysis will consider the control of the configuration of the arm as described by the deformed centerline and generalized Darboux vector (rather than just the end of the arm or a segment of the arm, for example). Specifically, such a configuration will be given by the set of functions $\{\kappa(\mathfrak{s}), \kappa'(\mathfrak{s}), \tau(\mathfrak{s}), \lambda(S)\}$, where Eq. (4.8) and Assumption 7 relate the extension parameter $\lambda(S)$ with the cross section parameter $\mathfrak{a}(S)$.

5.1 Inverse Kinematics. For the inverse kinematics problem the configuration of the octopus's arm is given in terms of the functions $\kappa(\mathfrak{s})$, $\kappa'(\mathfrak{s})$, $\tau(\mathfrak{s})$, and $\lambda(S)$, and the actuation variables are the strains in the various muscle groups. It will be assumed that the fibers of various groups are present coincidently at all points in the arm. Accordingly, we will calculate the strains at each point in the arm in the directions of the various groups.

We set ϵ_L, ϵ_{T1}, ϵ_{T2}, ϵ_{H1}, and ϵ_{H2} to be the strains in the directions of the longitudinal, oral-aboral and lateral transversal, and right and left helicoidal groups, respectively. Thus,

$$\epsilon_L = \mathbf{d}_3 \cdot \mathbf{E}(\mathbf{d}_3)$$

$$\epsilon_{T1} = \mathbf{d}_1 \cdot \mathbf{E}(\mathbf{d}_1)$$

$$\epsilon_{T2} = \mathbf{d}_2 \cdot \mathbf{E}(\mathbf{d}_2)$$

$$\epsilon_{H1} = \hat{\mathbf{n}}_c \cdot \mathbf{E}(\hat{\mathbf{n}}_c)$$

$$\epsilon_{H2} = \hat{\mathbf{n}}_{cc} \cdot \mathbf{E}(\hat{\mathbf{n}}_{cc}) \tag{5.1}$$

where $\hat{\mathbf{n}}_c$ and $\hat{\mathbf{n}}_{cc}$ are unit vectors pointing at the directions of the right and left coiled helicoidal muscle fibers, respectively. It assumed that in the reference configuration the helicoidal fibers are at 45 deg angle to the centerline.[2] Thus

$$\hat{\mathbf{n}}_c = \left\{ -\frac{rY}{A}, \frac{r^{-1}X}{A}, \frac{1}{\sqrt{2}} \right\}^T$$

$$\hat{\mathbf{n}}_{cc} = \left\{ \frac{rY}{A}, -\frac{r^{-1}X}{A}, \frac{1}{\sqrt{2}} \right\}^T \tag{5.2}$$

where $A = \sqrt{2}\sqrt{r^2Y^2 + r^{-2}X^2}$, and $r := a_0/b_0$ was defined following Assumption 7.

It is noted that by Assumption 7, $\epsilon_{T1} = \epsilon_{T2}$, and so it is natural to define the vector field

$$\boldsymbol{\epsilon}(X,Y,S) = \{\epsilon_{T1}(X,Y,S), \epsilon_L(S), \epsilon_{H1}(X,Y,S), \epsilon_{H2}(X,Y,S)\}^T \tag{5.3}$$

that contains the values of the analog of the actuation variables controlling the configuration of the arm.

For the inverse kinematics problem, we seek a mapping Ψ that acts on the set of functions $\{\kappa(\mathfrak{s}), \kappa'(\mathfrak{s}), \tau(\mathfrak{s}), \lambda(S)\}$ and gives $\boldsymbol{\epsilon}$, so

$$\boldsymbol{\epsilon}(X,Y,S) = \Psi(\kappa(\mathfrak{s}), \kappa'(\mathfrak{s}), \tau(\mathfrak{s}), \lambda(S), X, Y, S) \tag{5.4}$$

By using Eq. (4.13) we find that

$$\begin{Bmatrix} \epsilon_{T1} \\ \epsilon_L \\ \epsilon_{H1} \\ \epsilon_{H2} \end{Bmatrix} = [\mathbf{A}] \begin{Bmatrix} E_{11} \\ E_{33} \\ E_{13} \\ E_{23} \end{Bmatrix} \tag{5.5}$$

where

$$[\mathbf{A}] = \begin{bmatrix} 1 & 0 & 0 & 0 \\ 0 & 1 & 0 & 0 \\ \frac{1}{2} & \frac{1}{2} & -\sin\theta & \cos\theta \\ \frac{1}{2} & \frac{1}{2} & \sin\theta & -\cos\theta \end{bmatrix} \tag{5.6}$$

where $\sin\theta = (a_0^2 Y/\sqrt{b_0^4 X^2 + a_0^4 Y^2})$ and $\cos\theta = (b_0^2 X/\sqrt{b_0^4 X^2 + a_0^4 Y^2})$.

We define a nonlinear function $\mathbf{h}$ that takes the configuration parameters and gives the four strain components $(E_{11}, E_{33}, E_{13}, E_{23}) = \mathbf{h}(\kappa, \kappa', \tau, \lambda)$. By Eq. (4.14) we have

$$\mathbf{h}(\kappa,\kappa',\tau,\lambda) = \frac{1}{2} \begin{Bmatrix} \mathfrak{a}^2 - 1 \\ (\mathfrak{a}\lambda\kappa Y - \mathfrak{a}\lambda\kappa' X + \lambda)^2 + (\mathfrak{a}' Y + \mathfrak{a}\lambda\tau X)^2 + (\mathfrak{a}' X - \mathfrak{a}\lambda\tau Y)^2 - 1 \\ \mathfrak{a}\mathfrak{a}' X - \tau Y \\ \mathfrak{a}\mathfrak{a}' Y + \tau X \end{Bmatrix} \tag{5.7}$$

Hence, the inverse kinematics mapping Ψ is given by

$$\Psi = \mathbf{A} \circ \mathbf{h} \tag{5.8}$$

5.2 Forward Kinematics. The forward kinematic problem is concerned with the inverse $\Phi = \Psi^{-1}$ of the mapping Ψ defined above. Since the analogs of the joint parameters in our case are the strain fields within the arm, one might expect that the domain on which Ψ is defined is the collection of all continuous independent strain fields

$$\{(E_{11}(X,Y,S), E_{33}(X,Y,S), E_{13}(X,Y,S), E_{23}(X,Y,S))\} \tag{5.9}$$

However, this cannot hold true because not all strain fields correspond to continuous configurations of the arms. In fact, if a tensor field F_{ij} is indeed the gradient of a configuration of the arm, i.e., $F_{ij} = \partial x_i/\partial X_j$, then it must satisfy the compatibility condition

$$\frac{\partial F_{ij}}{\partial X_p} = \frac{\partial F_{ip}}{\partial X_j} = \frac{\partial^2 x_i}{\partial X_j \partial X_p} \tag{5.10}$$

Furthermore, it is clear that a generic configuration induced by a compatible strain field need not satisfy necessarily the assumptions we made in Sec. 3.1. For example, not every continuous configuration of the arm necessarily satisfies our assumption that the cross sections remain plane and perpendicular to the centerline. Furthermore, using Eq. (4.14), we find that the strain fields satisfy the constraint

$$E_{13}X + E_{23}Y = \mathfrak{a}\frac{d\mathfrak{a}}{dS}(X^2 + Y^2) \tag{5.11}$$

Thus, our analysis of the forward kinematics of the arm will lead us to the conclusion that the values of the strain at two points (X_1, Y_1, S_0) and (X_2, Y_2, S_0) in a cross section S_0 that are not on the centerline determine the values of $\mathfrak{a}(S_0)$, $d\mathfrak{a}/dS(S_0)$, $\kappa(\mathfrak{s}_0)$, $\kappa'(\mathfrak{s}_0)$, $\tau(\mathfrak{s}_0)$, and $\lambda(S_0)$, with some additional consistency conditions.

Noticing that the transformation $\mathbf{A}$ is singular and using

$$\frac{dE_{11}}{dS} = \frac{d}{dS}\frac{1}{2}(\mathfrak{a}^2 - 1) = \mathfrak{a}\mathfrak{a}' \tag{5.12}$$

and $\epsilon_{T1} = E_{11}$, we have

$$\begin{Bmatrix} \epsilon_{T1} \\ \epsilon_L \\ \epsilon_{H1} \\ \frac{d\epsilon_{T1}}{dS} \end{Bmatrix} = \begin{bmatrix} 1 & 0 & 0 & 0 \\ 0 & 1 & 0 & 0 \\ \frac{1}{2} & \frac{1}{2} & -\sin\theta & \cos\theta \\ 0 & 0 & \frac{X}{X^2+Y^2} & \frac{Y}{X^2+Y^2} \end{bmatrix} \begin{Bmatrix} E_{11} \\ E_{33} \\ E_{13} \\ E_{23} \end{Bmatrix} \tag{5.13}$$

where now, the transformation is invertible.

The inverse of Eq. (5.13) will give the vector $\{E_{11}, E_{33}, E_{13}, E_{23}\}$ in terms of the modified strain functions vector $\left\{\epsilon_{T1}, \epsilon_L, \epsilon_{H1}, \frac{d\epsilon_{T1}}{dS}\right\}$. In order to represent the configuration parameters $\{\kappa, \kappa', \tau, \lambda, a_1, a_2\}$ in terms of the strain functions—the forward kinematics mapping—we use Eq. (4.14) together with Eq. (5.13) to obtain

[2]The generalization to any other pitch angle is straightforward.

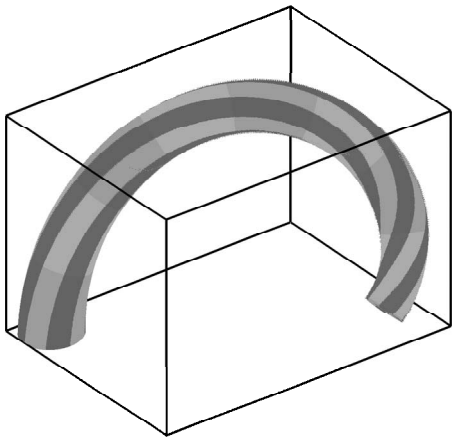

Fig. 4 Illustration of the arm's configuration depicted by Eq. (6.1)

$$a_1 = a_2 = \mathfrak{a} = \sqrt{2\epsilon_{T1} + 1} \tag{5.14}$$

$$\tau = \frac{(a_0^2 - b_0^2)XY}{b_0^2X^2 + a_0^2Y^2}\epsilon'_{T1} + \frac{\sqrt{b_0^4X^2 + a_0^4Y^2}}{2(b_0^2X^2 + a_0^2Y^2)}(2\epsilon_{H1} - \epsilon_{T1} - \epsilon_L) \tag{5.15}$$

$$\kappa\mathfrak{a}Y - \kappa'\mathfrak{a}X = \frac{\sqrt{2\epsilon_L - (\mathfrak{a}'Y + \mathfrak{a}\tau\lambda X)^2 - (\mathfrak{a}'X - \mathfrak{a}\tau\lambda Y)^2 + 1}}{\lambda} - 1 \tag{5.16}$$

Since none of the configuration parameters are functions of X or Y, we find that the expressions on the right hand sides of Eqs. (5.14) and (5.15) depend only on S. Thus, the independence of these expressions on X and Y, originating from the kinematical assumptions made, may be used as conditions for the in-plane strain fields to be compatible with some configuration.

To find τ, κ, and κ', we evaluate Eqs. (5.15) and (5.16) at two points in a cross section. For simplicity, we choose to evaluate the strain functions in Eq. (5.15) at $X=a_0$, $Y=0$, and thus we obtain

$$\tau(S) = \frac{1}{a_0}(2\epsilon_{H1}(a_0,0,S) - \epsilon_{T1}(a_0,0,S) - \epsilon_L(a_0,0,S)) \tag{5.17}$$

Setting $X=0$, $Y=b_0$ and $X=a_0$, $Y=0$ alternatively in Eq. (5.16), we obtain

$$\kappa(S) = \frac{\sqrt{2\epsilon_L(0,b_0,S) - (\mathfrak{a}'^2(S) + \tau^2(S)\lambda(S))b_0^2 + 1} - \lambda(S)}{\mathfrak{a}(S)\lambda(S)b_0} \tag{5.18}$$

$$\kappa'(S) = \frac{\lambda(S) - \sqrt{2\epsilon_L(a_0,0,S) - (\tau^2(S)\lambda(S) + \mathfrak{a}'^2(S))a_0^2 + 1}}{\mathfrak{a}(S)\lambda(S)a_0} \tag{5.19}$$

To conclude, we recall from Eq. (4.8) that

$$\lambda(S) = \frac{1}{\mathfrak{a}^2(S)} \tag{5.20}$$

6 Example

To demonstrate the use of the model in computing the strains in the different muscle fibers, we consider the following configuration of the arm:

$$\kappa(S) = 5S, \quad \kappa'(S) = 2.7, \quad \tau(S) = 0.5S, \quad \lambda(S) = 1 \tag{6.1}$$

illustrated in Fig. 4. By substituting Eq. (6.1) into Eqs. (5.5) and (5.6), we obtain the following strain field:

$$\begin{Bmatrix} \epsilon_{T1} \\ \epsilon_L \\ \epsilon_{H1} \\ \epsilon_{H2} \end{Bmatrix} = \begin{Bmatrix} 0 \\ \frac{1}{2}[(1 - 2.7X + 5SY)^2 + 0.25S^2(X^2 + Y^2) - 1] \\ \frac{1}{2}\left(\epsilon_L + 0.25\frac{(a_0^2Y^2 + b_0^2X^2)}{\sqrt{Y^2a_0^4 + X^2b_0^4}}S\right) \\ \frac{1}{2}\left(\epsilon_L - 0.25\frac{(a^2Y^2 + b^2X^2)}{\sqrt{Y^2a_0^4 + X^2b_0^4}}S\right) \end{Bmatrix} \tag{6.2}$$

Computing the configuration parameters using Eqs. (5.14) and (5.17)–(5.20) and the strains in Eq. (6.2) will result in the same configuration parameters given in Eq. (6.1). Moreover, it is readily shown that Eq. (5.16) holds for all

$$(X,Y) \in \{X = \alpha a_0, \ \ Y = \beta b_0 | 0 \le \alpha \le 1, \ \ 0 \le \beta \le 1\}$$

7 Conclusion

Studied from the point of view of robot kinematics, the octopus's arm emerges as a sophisticated continuous robot that uses the incompressibility of the material composing it in order to control its shape in space. We have no physiological data to support the assumption we have made regarding the behavior of the arm as a rod with variable cross section. In addition, we cannot justify our assumptions on the basis of the ratio between the size of the cross section relative to the length of the arm. Nevertheless, it seems to us that in the proposed model, we were able to capture the essential aspects of the way the configuration of the arm is controlled. Hopefully, such analyses can inspire the constructions of efficient continuous robots.

Acknowledgment

This work was partially supported by the Paul Ivanier Center for Robotics Research and Production Management at Ben-Gurion University. The manuscript was written during the sabbatical visit of R. Segev to the Department of Mechanical and Aerospace Engineering at the University of California, San Diego, hosted by J. Goddard.

Appendix: Representation of the Arm's Configuration Using the Frenet–Serret Parameters

An alternative approach to the above description of the arm's configuration is based on the well known Frenet–Serret parameters (FS) [26] for a spatial curve represented by a vector function $\mathbf{r}_0(\mathfrak{s}) \in \mathbb{R}^3$, where $\mathfrak{s}$ is the arc length along the curve. It is recalled that for the case of nonvanishing curvature, a unique Frenet–Serret frame can be associated with each point on the curve. The Frenet–Serret orthonormal basis at a point S is given by

$$\mathbf{T} = \frac{d\mathbf{r}_0}{d\mathfrak{s}}, \quad \mathbf{N} = \frac{1}{\kappa_{\mathrm{FS}}}\frac{d\mathbf{T}}{d\mathfrak{s}}, \quad \mathbf{B} = \mathbf{T} \times \mathbf{N} \tag{A1}$$

where $\mathbf{T}$, $\mathbf{N}$, and $\mathbf{B}$ are referred to as the tangent, normal, and binormal vectors, respectively. (We omitted the dependence on $\mathfrak{s}$ for brevity.) The parameters κ_{FS} and τ_{FS}, which are the curvature and the torsion, respectively, are defined by

$$\kappa_{\mathrm{FS}} = \left\| \frac{d\mathbf{T}}{d\mathfrak{s}} \right\|, \quad \tau_{\mathrm{FS}} = \frac{d\mathbf{N}}{d\mathfrak{s}} \cdot \mathbf{B} \tag{A2}$$

It can be shown that the curvature and torsion functions uniquely define an inextensible spatial curve up to a rigid body displacement [26]. The Frenet–Serret triads satisfy the differential equations

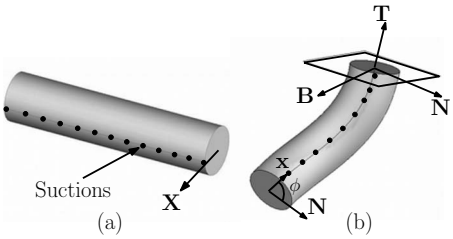

Fig. 5 (*a*) Reference configuration; (*b*) current configuration

$$\frac{d\mathbf{T}}{ds} = \kappa_{\mathrm{FS}}\mathbf{N}$$

$$\frac{d\mathbf{N}}{ds} = -\kappa_{\mathrm{FS}}\mathbf{T} + \tau_{\mathrm{FS}}\mathbf{B}$$

$$\frac{d\mathbf{B}}{ds} = -\tau_{\mathrm{FS}}\mathbf{N} \tag{A3}$$

The Frenet–Serret triads describe the geometry of the deformed centerline. In order to describe the configuration of the arm completely, we need to account for the stretch λ, the in-plane deformation, and the twist of the arm about the centerline. In order to describe the twist, we define a parameter ϕ, the angle between the normal unit vector $\mathbf{N}$, and the image $\mathbf{g}_1$ of the vector $\mathbf{G}_1$ (see Fig. 5).

Given the set $\{\kappa, \kappa', \tau\}$, when $\kappa'^2 + \kappa^2 \neq 0$, one can find the corresponding FS parameters by

$$\kappa_{\mathrm{FS}} = \sqrt{\kappa'^2 + \kappa^2} \tag{A4}$$

$$\tau_{\mathrm{FS}} = \tau + \frac{1}{(\kappa'^2 + \kappa^2)^{3/2}}\left(\kappa\frac{d\kappa'}{ds} - \kappa'\frac{d\kappa}{ds}\right) \tag{A5}$$

$$\phi = \cos^{-1}\left(\frac{\kappa'}{\sqrt{\kappa'^2 + \kappa^2}}\right) = \sin^{-1}\left(\frac{-\kappa}{\sqrt{\kappa'^2 + \kappa^2}}\right) \tag{A6}$$

References

[1] Levinson, Y., 2008, "On the Kinematics of the Octopus's Arm," MS thesis, Department of Mechanical Engineering, Ben-Gurion University, Beer-Sheva, Israel.

[2] Fahimi, F., Ashrafiuon, H., and Nataraj, C., 2002, "An Improved Inverse Kinematic and Velocity Solution for Spatial Hyper-Redundant Robots," IEEE Trans. Rob. Autom., **18**(1), pp. 103–107.

[3] Sujan, V. A., and Dubowsky, S., 2004, "Design of a Lightweight Hyper-Redundant Deployable Binary Manipulator," ASME J. Mech. Des., **126**, pp. 29–39.

[4] Yamada, H., and Hirose, S., 2006, "Study on the 3D Shape of Active Cord Mechanism," Proceedings of the 2006 IEEE International Conference on Robotics and Automation (ICRA), pp. 2890–2895.

[5] Gallardo, J., Orozco, H., Rico, J. M., and Gonzalez-Galvan, E. J., 2009, "A New Spatial Hyper-Redundant Manipulator," Rob. Comput.-Integr. Manufact., **25**, pp. 703–708.

[6] Chapelle, F., and Bidaud, Ph., 2006, "Evaluation Functions Synthesis for Optimal Design of Hyper-Redundant Robotic Systems," Mech. Mach. Theory, **41**, pp. 1196–1212.

[7] Dasgupta, B., Gupta, A., and Gingla, E., 2009, "A Variational Approach to Path Planning for Hyper-Redundant Manipulators," Rob. Auton. Syst., **57**, pp. 194–201.

[8] Trivedi, D., Rahn, C. D., Kier, W. M., and Walker, I. D., 2008, "Soft Robotics: Biological Inspiration, State of the Art and Future Research," Applied Bionics and Biomechanics, **5**, pp. 99–117.

[9] Jones, B. A., and Walker, I. D., 2006, "Kinematics for Multisection Continuum Robots," IEEE Trans. Robot., **22**, pp. 43–55.

[10] Sugiyama, Y., and Hirai, Sh., 2006, "Crawling and Jumping by a Deformable Robots," Int. J. Robot. Res., **25**, pp. 603–620.

[11] Li, C., and Rahn, C. D., 2002, "Design of Continuous Backbone, Cable-Driven Robots," ASME J. Mech. Des., **124**, pp. 265–271.

[12] Wakamatsu, H., Arai, E., and Hirai, Sh., 2006, "Knotting/Unknotting Manipulation of Deformable Linear Objects," Int. J. Robot. Res., **25**, pp. 371–395.

[13] Moll, M., and Kavraki, L. E., 2006, "Path Planning for Deformable Linear Objects," IEEE Trans. Robot., **22**, pp. 625–636.

[14] Saha, M., and Isto, P., 2006, "Motion Planning for Robotic Manipulation of Deformable Linear Objects," Proceedings of the 2006 IEEE International Conference on Robotics and Automation (ICRA), pp. 2478–2484.

[15] Theetten, A., Grisoni, L., Andriot, C., and Barsky, B., 2008, "Geometrically Exact Dynamic Splines," Comput.-Aided Des., **40**, pp. 35–48.

[16] Jingzhou, Y., Jason, P., and Abdel-Malek, K., 2006, "A Hyper-Redundant Continuous Robot," Proceedings of the 2006 IEEE International Conference on Robotics and Automation (ICRA), pp. 1854–1859.

[17] Yekutieli, Y., Sagiv-Zohar, R., Aharonov, R., Engel, Y., Hochner, B., and Flash, T., 2005, "Dynamic Model of the Octopus Arm I: Biomechanics of the Octopus Reaching Movement," J. Neurophysiol., **94**, pp. 1443–1458.

[18] Yekutieli, Y., Sagiv-Zohar, R., Hochner, B., and Flash, T., 2005, "Dynamic Model of the Octopus Arm II: Control of Reaching Movements," J. Neurophysiol., **94**, pp. 1459–1468.

[19] Chirikjian, G. S., and Burdick, J. W., 1995, "Kinematically Optimal Hyper-Redundant Manipulator Configurations," IEEE Trans. Rob. Autom., **11**(6), pp. 794–806.

[20] Zanganeh, K. E., and Angeles, J., 1995, "Inverse Kinematics of Hyper-Redundant Manipulators Using Splines," Proceedings of the IEEE International Conference on Robotics and Automation, Vol. 3, URL http://dx.doi.org/10.1109/ROBOT.1995.525679.

[21] Boyer, F., Porez, M., and Khalil, W., 2006, "Macro-Continuous Computed Torque Algorithm for a Three-Dimensional Eel-Like Robot," IEEE Trans. Robot., **22**(4), pp. 763–775.

[22] Antman, S. S., 2006, "A Priori Bounds on Spatial Motions of Incompressible Nonlinearly Elastic Rods," Journal of Hyperbolic Differential Equations, **3**(3), pp. 481–504.

[23] Kier, W. M., and Smith, K. K., 1985, "Tongues, Tentacles and Trunks: The Biomechanics of Movement in Muscular-Hydrostats," Zool. J. Linn. Soc., **83**, pp. 307–324.

[24] Kier, W., and Stella, M., 2007, "The Arrangement and Function of Octopus Arm Musculature and Connective Tissue," J. Morphol., **268**, pp. 831–843.

[25] Villaggio, P., 1997, *Mathematical Models for Elastic Structures*, Cambridge University Press, Cambridge, England.

[26] Struik, D., 1961, *Lectures on Classical Differential Geometry*, Addison-Wesley, Reading, MA.